

IMPROVING WATER ICE CLOUD MODELLING IN THE LMD GLOBAL CLIMATE MODEL : MARS CLIMATE SOUNDER DATA COMPARISONS.

A. Pottier, (alizee.pottier@latmos.ipsl.fr) *Laboratoire Atmosphères, Milieux, Observations Spatiales, Guyancourt, France*, **F. Montmessin**, *Laboratoire Atmosphères, Milieux, Observations Spatiales, Guyancourt, France*, **F. Forget**, *Laboratoire de Météorologie Dynamique, UPMC, Paris, France*, **T. Navarro**, *Laboratoire de Météorologie Dynamique, UPMC, Paris, France*.

Introduction

The Global Climate Model (GCM) from the Laboratoire de Météorologie Dynamique (LMD) is in constant improvement. Much effort was put in improving the microphysics of clouds and their radiative interaction with the atmosphere (Montmessin et al. (2004), Madeleine et al. (2012), Navarro et al. (2013)). However, implementing radiatively active clouds added much instability in its description of the martian water cycle. Indeed, water clouds, that is to say, water ice floating in the air, in the case of Mars, are linked to the water vapor distribution in the atmosphere of the planet and the temperature profiles. There is constant feedback between these three elements.

That is why it is important to intercompare what we know about the spatial and temporal distribution of clouds, water vapor and temperature with model runs. The data is given by multiple orbiters that have gathered lots of data over years of martian observation by orbiters. The focus of the study presented here is the Mars Climate Sounder water ice cloud data, in its fourth release.

Mars Climate Sounder Data

The last release of the Mars Climate Sounder data was provided by Luca Montabone. For the study of the Martian Water Cycle, they hold the distribution of the water ice cloud opacity daily and nightly for nearly full martian years. The wavelength at which these opacities are given is $\lambda_{ice} = 843 \text{ cm}^{-1}$ (11.9 μm) for water ice (McCleese et al. (2010)). The dust opacity is also given at $\lambda_{dust} = 463 \text{ cm}^{-1}$ (21.6 μm).

Data currently available for the last releases cover Martian years 28, 29, 30 and 31. GCM dust scenarios, which are needed to compute one particular year, are available for years 28, 29, and 30, as for now (other years exist, of course, but are not relevant to that MCS study).

LMD Global Climate Model runs

The Martian GCM developed at the LMD (Laboratoire de Météorologie Dynamique) was adapted to produce output having the same type as MCS data. This was

used by writing to output files, at each level, water ice cloud opacity at the reference wavelength λ_{ice} .

This opacity was calculated using the information from Kleinböhl et al. (2009) about the MCS retrievals, that did not take scattering into account at the time:

$$\kappa(z) = \tau_{vis}(z) \frac{Q_{ref_{IR}}}{Q_{ref_{vis}}} \frac{1 - \omega_{ref_{IR}}}{\frac{rT}{g} \log \frac{p_n}{p_{n+1}}} \quad (1)$$

where τ_{vis} is the optical depth of a given aerosol at the reference visible wavelength used for GCM computations ($\lambda_{ref_{vis}} = 670 \text{ nm}$), Q the absorption efficiencies of the visible and infrared reference wavelengths, $\omega_{ref_{IR}}$ the single scattering albedo at the wavelength of MCS water ice retrievals, and we divide by $|dz| = \frac{rT}{g} \log \frac{p_n}{p_{n+1}}$ with r the gas constant relative to a gas, to obtain the result $\kappa(z)$, the water ice cloud opacity at a given level.

Dust opacity at the same wavelength used by MCS retrievals was also produced in these runs.

Results

Here we will show some results for Martian year 29. Other years are also being studied: during Martian year 28, there was a huge dust storm that might explain discrepancies between data and the global climate model.

0.1 Vertical distribution

We can look at the clouds' extension in height in these maps of the zonal mean of water ice cloud opacity during the night (figure 1) and the day (figure 2), as seen by MCS and as modelled by the GCM, for latitude 10 °N. The aphelion cloud belt is clearly visible between roughly solar longitudes $L_s = 40^\circ$ and $L_s = 160^\circ$, that is to say northern spring and summer.

We can see the lack of MCS data under the upper part of the aphelion belt for the daytime clouds, as MCS has trouble retrieving water ice opacity when the clouds are too thick. They seem to have better luck during the night. However, for GCM data, the mean cloud opacity reaches $5 \times 10^{-3} \text{ km}^{-1}$ for the whole lifespan of the belt, whereas observed opacity only reaches that value sporadically in daytime, and in nighttime peaks at $3 \times 10^{-3} \text{ km}^{-1}$ only. The simulated aphelion belt reaches

Water ice clouds: MCS data and LMD GCM runs

lower than the observed one, and its gravity center seems closer to the surface.

During northern fall, and in the night, clouds seem to lose gradually height on MCS data, whereas they go up in the GCM run. They have the same decreasing evolution during northern winter. At this time, the bulge of clouds observed at around 10 Pa is a bit thicker (at around $2 \times 10^{-3} \text{ km}^{-1}$), less vertically extended and more stable than the one modelled.

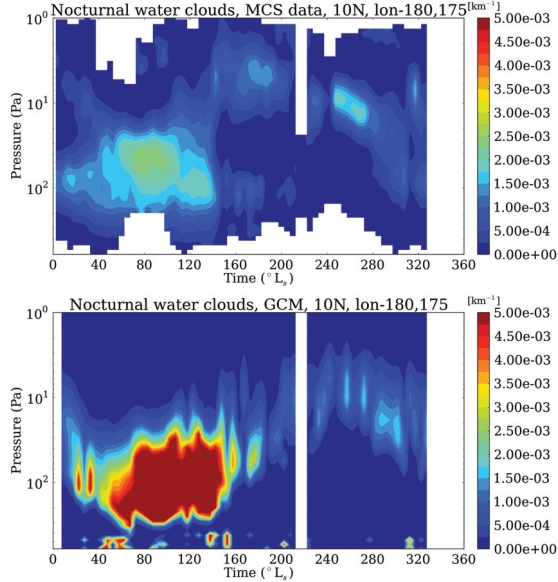


Figure 1: Zonally averaged cloud cover during nighttime, up: as seen by MCS, down: as computed by the GCM. 10°N : aphelion belt is visible.

Let us look closer to the poles. Figure 3 is similar to the previous ones but shows the vertical extension of the water ice clouds for a latitude of 75°N , and figure 4 does the same for 75°S . We can see that a thick cloud cover is modelled, except in the respective summer seasons ($L_s = 90 - 180^\circ$ for northern hemisphere, $L_s = 270 - 360^\circ$ for southern hemisphere) of the two poles, which is compatible with the existing polar hoods. The lack of data near the ground may cripple us, but we can still see there are problems with our modelling of those hoods. They seem not to extend upwards enough if we compare them to the observed ones. And they still seem too thick, as far as we can see. Between $L_s = 160$ and 320° , in the north, mean opacity values quickly (around some hundreds of Pa) reach zero in the model while they remain as high as $2 \times 10^{-3} \text{ km}^{-1}$ near 10 Pa in the observations. To a lesser extent, the same phenomenon is visible in the southern burst of clouds around the northern fall equinox. What is more, the observed burst reaches its maximum around the 100 Pa pressure level, while the modelled clouds increase gradually as we get

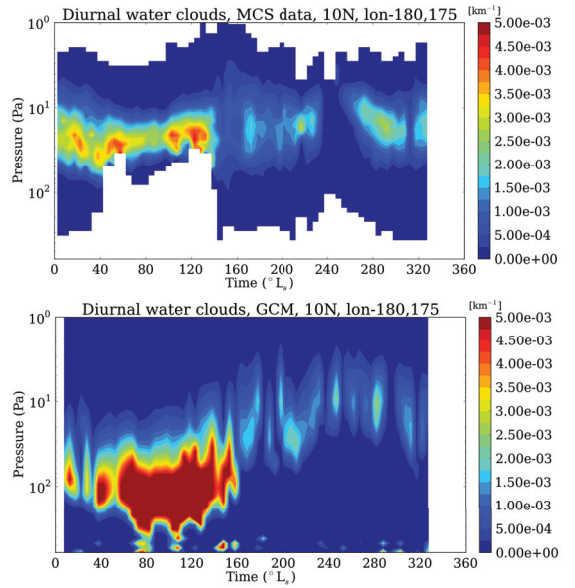


Figure 2: Zonally averaged cloud cover during daytime, up: as seen by MCS, down: as computed by the GCM. 10°N : aphelion belt is visible.

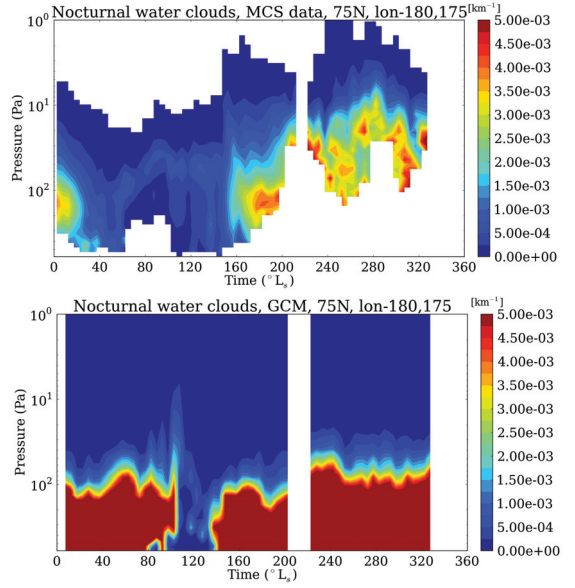


Figure 3: Zonally averaged cloud cover during the night, up: as seen by MCS, down: GCM run. 75°N .

Water ice clouds: MCS data and LMD GCM runs

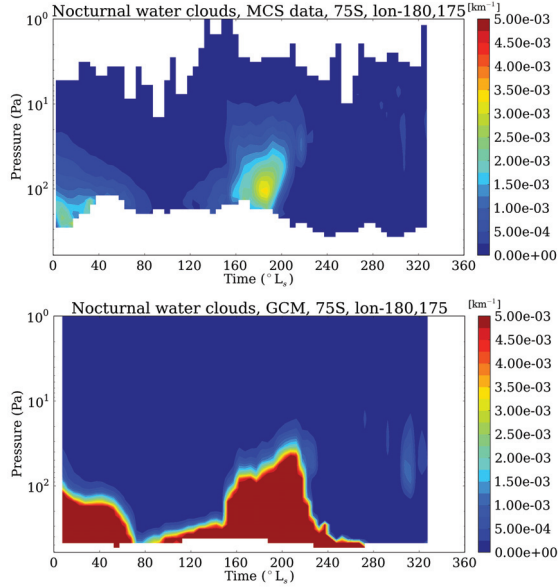


Figure 4: Zonally averaged cloud cover during the night, up: as seen by MCS, down: GCM run. 75 °S.

closer to the ground (which is more visible with maps with a more extended color palette).

0.2 Cloud cover: latitude and seasons

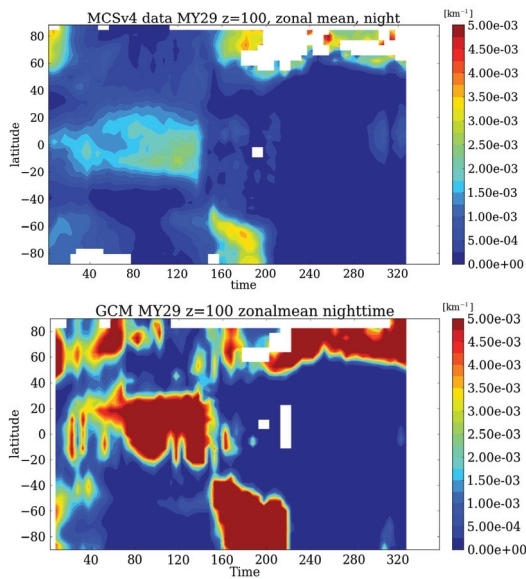


Figure 5: Zonally averaged cloud cover during the night, up: as seen by MCS, down: GCM run. The water ice cloud cover is shown at the 100 Pa level.

We can see on figure 5 water ice clouds at the level of 100 Pa (which is about 20 km). Clouds are on the whole thicker in the GCM run at this pressure level.

There are pseudo-oscillations with a period of several days (5 or 6 according to more detailed maps which are not presented here). These are clearly not so pronounced in MCS observations and need to be addressed and understood.

The average cloud cover at 100 Pa seems globally accurate on the whole, except for the underestimation by the model of the transient cloud cover at middle latitudes at the end of the year.

0.3 Dust repartition and cloud activity

Water cloud activity is related to the amount of aerosols present in Mars' atmosphere. Indeed, ice crystals start to grow on condensation nuclei during the process of nucleation. The inclusion of microphysics takes that into account, and dust is part of the model as a tracer.

Dust as it could be seen by MCS is also modelled in the GCM. Here is (figure 6) an example comparison that can be related to the water ice cloud distribution previously seen on figure 1. The higher clouds seen by MCS during the end of northern summer and beginning of fall are clearly related to scatterers that were observed at the same height and which are not present in the GCM run. On the whole, except for these detached layers of dust, the GCM correctly simulates MCS dust observations.

This study might be even more exciting for Mars Year 28, which holds a global dust storm.

Conclusion and prospects

The work described here is still in progress. As we have seen, much remains to be understood and thoroughly explored.

First of all, most of the time, the sheer amount of water ice is lower in MCS data than in GCM simulations. MCS data is intrinsically biased toward lighter clouds. That could explain some of the major differences with our model runs.

The study of other martian years has also begun, and we will most probably learn much from their similarities and differences.

Access was gained to the last release and software to retrieve information about water vapor in the data from the OMEGA spectro-imager aboard Mars Express, on orbit around Mars since 2003, with extended missions until 2012. With the help of Luca Maltagliati's retrieval process, which he developed during his PhD thesis, the goal is to extend the current knowledge (Maltagliati et al. (2011)) about the water vapor distribution with the latest orbits from the orbiter.

REFERENCES

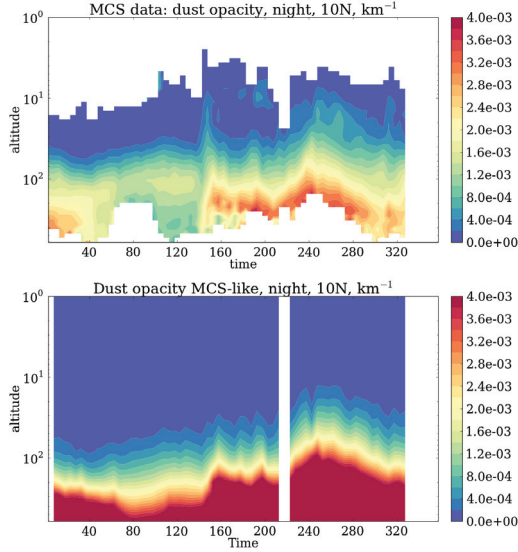


Figure 6: Zonally averaged cloud cover during the night, up: as seen by MCS, down: GCM run. The water ice cloud cover is shown at the 100 Pa level.

The water vapor distribution in problematic areas as observed by OMEGA, correlated with our knowledge of the cloud distribution, which will be extended, is bound to help us find out where the problems lie in our cloud models.

References

- Kleinböhl, A., Schofield, J. T., Kass, D. M., Abdou, W. A., Backus, C. R., Sen, B., Shirley, J. H., Law-
son, W. G., Richardson, M. I., Taylor, F. W., Teanby, N. A., and McCleese, D. J. (2009). Mars Climate Sounder limb profile retrieval of atmospheric temperature, pressure, and dust and water ice opacity. *Journal of Geophysical Research (Planets)*, 114:10006.
- Madeleine, J.-B., Forget, F., Millour, E., Navarro, T., and Spiga, A. (2012). The influence of radiatively active water ice clouds on the Martian climate. "Geophysical Research Letters", 39:23202.
- Maltagliati, L., Titov, D. V., Encrenaz, T., Melchiorri, R., Forget, F., Keller, H. U., and Bibring, J.-P. (2011). Annual survey of water vapor behavior from the OMEGA mapping spectrometer onboard Mars Express. *Icarus*, 213:480–495.
- McCleese, D. J., Heavens, N. G., Schofield, J. T., Abdou, W. A., Bandfield, J. L., Calcutt, S. B., Irwin, P. G. J., Kass, D. M., Kleinböhl, A., Lewis, S. R., Paige, D. A., Read, P. L., Richardson, M. I., Shirley, J. H., Taylor, F. W., Teanby, N., and Zurek, R. W. (2010). Structure and dynamics of the Martian lower and middle atmosphere as observed by the Mars Climate Sounder: Seasonal variations in zonal mean temperature, dust, and water ice aerosols. *Journal of Geophysical Research (Planets)*, 115:12016.
- Montmessin, F., Forget, F., Rannou, P., Cabane, M., and Haberle, R. M. (2004). Origin and role of water ice clouds in the Martian water cycle as inferred from a general circulation model. *Journal of Geophysical Research (Planets)*, 109:10004.
- Navarro, T., Madeleine, J.-B., Forget, F., Spiga, A., Millour, E., and Montmessin, F. (2013). Global Climate Modeling of the Martian water cycle with improved microphysics and radiatively active water ice clouds. *ArXiv e-prints*.